Mammalian BLM helicase is critical for integrating multiple pathways of meiotic recombination

J. Kim Holloway, Meisha A. Morelli, Peter L. Borst, and Paula E. Cohen

Department of Biomedical Sciences, College of Veterinary Medicine, Cornell University, Ithaca, NY 14853

Bloom's syndrome (BS) is an autosomal recessive disorder characterized by growth retardation, cancer predisposition, and sterility. BS mutated (*Blm*), the gene mutated in BS patients, is one of five mammalian RecQ helicases. Although BLM has been shown to promote genome stability by assisting in the repair of DNA structures that arise during homologous recombination in somatic cells, less is known about its role in meiotic recombination primarily because of the embryonic lethality associated with *Blm* deletion. However, the localization of BLM protein on meiotic chromosomes together with evidence from yeast and other organisms implicates a role for BLM helicase in meiotic recombination events, prompting us to explore the meiotic phenotype of mice bearing a conditional mutant allele of *Blm*. In this study, we show that BLM deficiency does not affect entry into prophase I but causes severe defects in meiotic progression. This is exemplified by improper pairing and synapsis of homologous chromosomes and altered processing of recombination intermediates, resulting in increased chiasmata. Our data provide the first analysis of BLM function in mammalian meiosis and strongly argue that BLM is involved in proper pairing, synapsis, and segregation of homologous chromosomes; however, it is dispensable for the accumulation of recombination intermediates.

Introduction

In humans, mutation of the RecQ helicase Bloom's syndrome (BS) mutated (*BLM*) results in the carrier suffering from the rare autosomal recessive disorder, BS. BS is characterized by sunlight sensitivity, immunodeficiency, and cancer predisposition (German, 1993; Payne and Hickson, 2009), and sufferers from BS will have a severely decreased life expectancy. Cells from BS patients exhibit severe cytogenetic abnormalities, as characterized by increased sister chromatid exchange, chromosome fragmentation, and translocations that arise in the absence of BLM as a result of derepressed crossing over during mitotic recombination (Payne and Hickson, 2009). In mammalian cells, BLM exists in a complex with topoisomerase IIIα and BLAP75 (Yin et al., 2005), and it is thought that this latter component acts to recruit topoisomerase IIIα/BLM to Holliday junction substrates to promote their dissolution (Wu et al., 2006).

To date, there is no information on the impact of BLM in mammalian meiosis; however, BS patients exhibit varying levels of infertility (German, 1995; Ellis and German, 1996), indicating that this protein may play an important role in meiotic progression.

During meiosis, the ultimate goal of crossing over during prophase I is to tether homologous chromosomes together until the first meiotic division, when they must segregate equally into daughter cells that then enter meiosis II. Appropriate segregation is ensured by the correct repair of double-strand breaks (DSBs) either as crossover (CO) events, manifested as chiasmata, which serve to maintain homologous chromosome interactions through metaphase I, or as non-COs. CO number and placement are extremely tightly regulated among all eukaryotes. DSB ends are resected to form 3′ single-stranded tails that assemble the RecA homologues Rad51 and Dmc1 to promote homology searching and strand exchange (Shinohara and Shinohara, 2004). Subsequent formation of recombination intermediates (or joint molecules [JMs]) depends on the nature of the exchange event (Bishop and Zickler, 2004) and remains poorly understood in mammals. These intermediates presumably include the double-Holliday junctions that have been most

Correspondence to Paula E. Cohen: paula.cohen@cornell.edu

Abbreviations used in this paper: BLM, BS mutated; BS, Bloom's syndrome; CKO, conditional knockout; CO, crossover; DSB, double-strand break; DSBR, DSB repair; JM, joint molecule; mcJM, multichromatid JM.

The Rockefeller University Press $30.00
J. Cell Biol. Vol. 188 No. 6 779–789
www.jcb.org/cgi/doi/10.1083/jcb.200909048

consistently linked with reciprocal recombination or CO events in most meiotic species, including budding yeast and mice. The only data we have about the major CO pathway are defined in budding yeast by the ZMM genes (*ZIP1-4*, *MSH4*, *MSH5*, and *MER3*; Bishop and Zickler, 2004; Börner et al., 2004; Shinohara et al., 2008). In mammals, several of these gene products, including TEX11 (the mammalian ZIP4 orthologue), MSH4, and MSH5, are also presumed to promote crossing over (Paquis-Flucklinger et al., 1997; de Vries et al., 1999; Edelmann et al., 1999; Kneitz et al., 2000), but the mechanism by which these CO/non-CO processes are differentiated is unclear in higher eukaryotes as a result of the early prophase I lethality of these cells.

Previous studies in budding yeast demonstrated that the yeast orthologue of mammalian BLM, Sgs1, together with Top3 and Rmi1 (the yeast orthologue of BLAP75), acts as an anti-CO factor at designated recombination sites to reduce axial associations and subsequent reciprocal exchange events (Rockmill et al., 2003). Thus, *sgs1* mutants exhibit reduced sporulation and spore viability, which is associated with increased axial associations between homologous chromosomes during prophase I and increased crossing over (Rockmill et al., 2003). More recently, a study in yeast has determined that Sgs1 plays a limited role in CO formation in wild-type cells but that under conditions of limited ZMM activity, *sgs1* mutation restores COs almost to wild-type levels (Jessop et al., 2006). Furthermore, Sgs1 can prevent aberrant crossing over by suppressing the formation of JMs that involve complex multichromatid duplex structures (Oh et al., 2007). This suggests that Sgs1 can act as a JM dissolution factor when faced with inappropriate DSB processing and/or the accumulation of nonproductive JMs, with proper accumulation of the ZMM proteins preventing the access of Sgs1 to early CO intermediates. Together with its known function in mitotic recombination, these observations suggest that BLM acts to suppress crossing over, which is similar to the proposed roles for Sgs1 in yeast.

The role of BLM in mammalian meiosis is not yet clearly defined. Male BS patients are sterile, and females have reduced fertility (Kauli et al., 1977; German, 1995). *Blm* is expressed at high levels in the mouse testis (Chester et al., 1998), and the protein is present from early prophase I (Moens et al., 2000). BLM localizes in discrete foci along meiotic chromosomes, increasing in number as homologous chromosomes pair and begin to synapse, and colocalizing with the RecA homologues DMC1 and RAD51 (Walpita et al., 1999; Moens et al., 2000). BLM is gradually lost from meiotic chromosome cores in early to mid-pachynema (Walpita et al., 1999).

Given the role of Sgs1 in yeast meiosis (Rockmill et al., 2003), together with the multiple lines of evidence showing a role for mammalian BLM in limiting recombination events in somatic cells, the aim of the current study was to more fully explore the role of BLM in mammalian meiosis and its interaction with other components of the recombination machinery. However, because mice harboring an inactivating mutation in *Blm* exhibit embryonic lethality at embryonic day (E) 13.5 (Chester et al., 1998), we used a mouse line carrying a conditional knockout (CKO) allele of *Blm*, which has been used successfully to create mice in which *Blm* is ablated specifically in the T cell lineage (Chester et al., 2006). The limited availability of *Cre* lines that express exclusively in meiotic germ cells in the mouse has hitherto precluded genetic analysis of BLM function during prophase I. To overcome this technical issue, we used *Tnap-cre* mice, one of only a handful of available *Cre* lines that express in mammalian germ cells (Lomelí et al., 2000). In the absence of BLM in spermatocytes during prophase I, complex multichromatid configurations were observed, and BLM appears to be essential for normal pairing, synapsis, and localization of the phosphorylated histone γH2AX at pachynema of prophase I. Interestingly, despite apparently normal progression of DSB repair (DSBR) events via the ZMM-defined pathway, *Blm* CKO spermatocytes show significantly increased numbers of chiasmata at diakinesis, suggesting an important and novel role for BLM in regulating recombination events via multiple pathways in mammalian germ cells. These experiments shed light on how multiple recombination pathways may be integrated to effect appropriate CO control, resulting in strict maintenance of CO numbers in mammalian germ cells.

Results

BLM and MLH3 have interconnected roles in prophase I

The BLM orthologue in yeast, Sgs1, has been proposed as an anti-CO factor, working as an antagonist to pro-CO factors such as MSH4–MSH5 and MLH1–MLH3 (Jessop et al., 2006; Oh et al., 2007). In yeast *msh5Δ* mutants, Sgs1 prevents the formation of double-Holliday junctions, and mutation of *SGS1* alleviates CO defects in both *msh5Δ* and *mlh3Δ* yeast mutants, indicating a delicate interplay between these two families of proteins, the anti- and pro-CO factors (Jessop et al., 2006; Oh et al., 2007). To define interconnected roles of BLM and MLH3 proteins in mouse meiosis, localization of BLM was performed on spermatocytes from both $Mlh3^{+/+}$ and $Mlh3^{-/-}$ animals (Fig. 1). Localization of BLM in zygonema is similar in both the $Mlh3^{+/+}$ and $Mlh3^{-/-}$ cells; however, by pachynema, BLM appears to persist on the chromosome cores of spermatocytes from $Mlh3^{-/-}$ males, whereas it has diminished to a few foci per chromosome in $Mlh3^{+/+}$. This suggests one of three possibilities: (1) MLH3 deficiency allows BLM to access previously restricted target sites, (2) BLM is recruited to facilitate crossing over via another recombination pathway, and/or (3) some global signal that triggers loss of BLM from synapsed chromosomes during mid-pachynema is absent in *Mlh3*-deficient spermatocytes. Either way, the apparent overaccumulation of BLM across the SC (and to some extent diffusely throughout the chromatin) would suggest that BLM localizes to sites above and beyond those that represent CO events.

Interestingly, markers for recombination intermediates remain similar to wild-type levels in Blm CKO spermatocytes

To assess the progression of meiotic DSBR events in *Blm* CKO mutant mice, immunofluorescent staining with an antibody against MSH4 was performed on meiotic chromosome spreads.

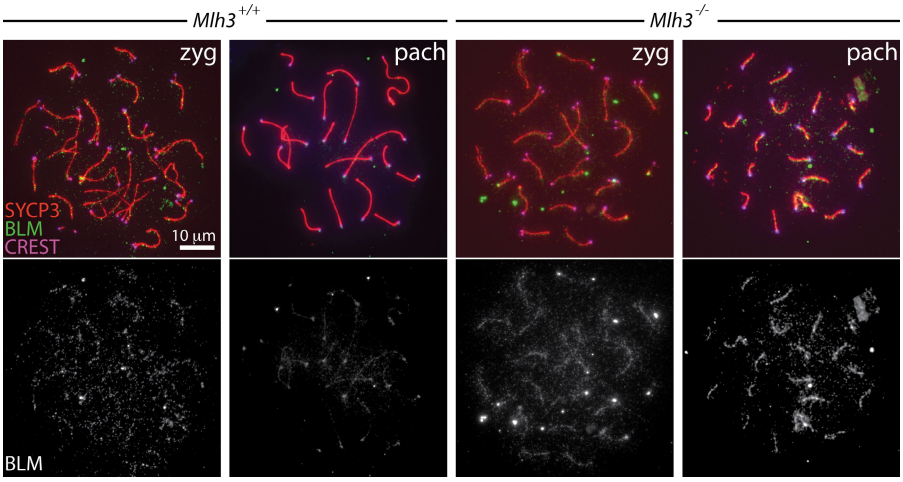

Figure 1. **BLM staining persists on *Mlh3*$^{-/-}$ pachytene spermatocyte chromosome cores.** Zygotene (zyg) and pachytene (pach) spermatocytes from both *Mlh3*$^{+/+}$ *and* *Mlh3*$^{-/-}$ mice stained with SYCP3 (red), BLM (green), and CREST (pink). BLM accumulates normally in zygonema in both cohorts of mice; however, it is still present in high numbers in pachynema in the *Mlh3*$^{-/-}$ cells but not in *Mlh3*$^{+/+}$ cells.

Spermatocytes from *Blm*$^{cko/neo}$ (CKO) and *Blm*$^{flox/neo}$ (control) accumulate MSH4 foci at a normal frequency (Fig. 2 A, P = 0.110). Coimmunostaining with antibodies against SYCP3 and MLH1 revealed that MLH1 focus numbers are also at normal levels in *Blm*$^{cko/neo}$ when compared with *Blm*$^{flox/neo}$ control spermatocytes (Fig. 2, B and C), suggesting that these initial steps in the CO pathway occur normally despite the absence of BLM. However, because of the incomplete excision previously reported in the *Tnap-cre* mice (Lomelí et al., 2000), which renders some spermatocytes BLM positive and some BLM negative, coimmunostaining was performed on chromosome spermatocyte spreads from both *Blm*$^{cko/neo}$ and *Blm*$^{flox/neo}$ mice, using antibodies against both BLM and MLH1 simultaneously (Fig. 2 D). Dual staining with MLH1 and BLM revealed that *Blm*$^{cko/neo}$ slides have cohorts of both BLM-positive and BLM-negative cells (Fig. 2 D, left), both of which localize MLH1 at wild-type levels. In addition to this staining, costaining of MLH1 and BLM was performed in the presence of SYCP3 staining, using the same secondary antibody to stain both MLH1 and SYCP3. This allows the MLH1 foci to be visualized as brighter spots of fluorescence on the chromosome cores (Fig. 2 D, right), demonstrating that in the absence of BLM staining on chromosome cores in *Blm*$^{cko/neo}$ spermatocytes, MLH1 still localizes at frequencies similar to those seen in spermatocytes from control and wild-type mice. Unfortunately, the fact that the anti-MSH4 and -BLM antibodies were both produced in rabbits precluded a similar comparison between *Blm*-intact and -excised testes for MSH4 accumulation. However, because the variation in MSH4 focus numbers was statistically indistinguishable between genotypes, we conclude that the absence of BLM has no effect on MSH4 frequency.

Chiasmata or chiasmata-like structures are elevated in *Blm* CKO mice

To assess chiasmata frequencies in the absence of BLM, air-dried diakinesis spreads were performed on *Blm*$^{cko/neo}$ and *Blm*$^{flox/neo}$ mice and stained with GIEMSA (Fig. 3, A–C). Significantly elevated numbers of chiasmata or chiasmata-like structures were recorded in diakinesis cells from *Blm*$^{cko/neo}$ mice compared with *Blm*$^{flox/neo}$ mice (Fig. 3 B, P = 0.0035). However, it is clear from the quantitation of individual cells that the distribution of chiasmata numbers follows a bimodal distribution, reflecting those cells containing the excised *Blm* allele (having elevated chiasmata numbers) and those containing the floxed *Blm* allele (having normal chiasmata numbers). Therefore, to confirm the increased chiasmata frequency, we also counted the number of chiasmata per chromosome for cells from both *Blm*$^{flox/neo}$ and *Blm*$^{cko/neo}$ mice (Fig. 3 C). The distribution of one, two, or three chiasmata chromosomes in the CKO mice was significantly different to those from the controls, with an increase in chromosomes containing three COs in cells from *Blm*$^{cko/neo}$ (P = 0.0053 by unpaired Welch's *t* test). In addition, cells from *Blm*$^{cko/neo}$ mice display abnormal chiasmata or chiasmata-like structures (Fig. 3 A, arrows). In these cells, there appear to be multiple CO structures along single chromosomes. In addition to these multiple structures, there were also cases of thin bridges of DNA between chromosomes seen in diakinesis spread cells from *Blm*$^{cko/neo}$ mice (Fig. 3 A, arrowhead), which were not observed in *Blm*$^{flox/neo}$ cells. Both of these aberrations in diakinesis cells suggest that the cells arrest at or before metaphase I.

Blm CKO spermatocytes display serious defects in pairing and synapsis

Yeast *sgs1* mutants exhibit altered synapsis (Rockmill et al., 2003), prompting the question of whether *Blm* CKO spermatocytes show similar aberrations. Immunostaining of pachytene spermatocytes revealed an increased frequency of cells with at least one asynaptic chromosome in *Blm*$^{cko/neo}$ mice compared with *Blm*$^{flox/neo}$ mice (5.4% and 0%, $n = 111$ and $n = 104$, respectively), as measured by SYCP1 and SYCP3 colocalization along meiotic chromosome cores (Fig. 4). This asynapsis appears to be a result of mispairing between nonhomologous chromosomes, as can be observed in Fig. 4 (middle, inset). In this example, SYCP3 marks the homologous chromosomes as expected in addition to regions of synapsis (that are also marked by SYCP1). However, individual sister chromatids rather than homologous chromosomes can also be seen to be stained with anti-SYCP3 antibodies (Fig. 4, gray). A cartoon is provided to interpret these complex configurations (Fig. 4, middle). This phenotype is similar to that seen in mutants for the cohesin component *Rec8*, in which SYCP3 also localizes along sister

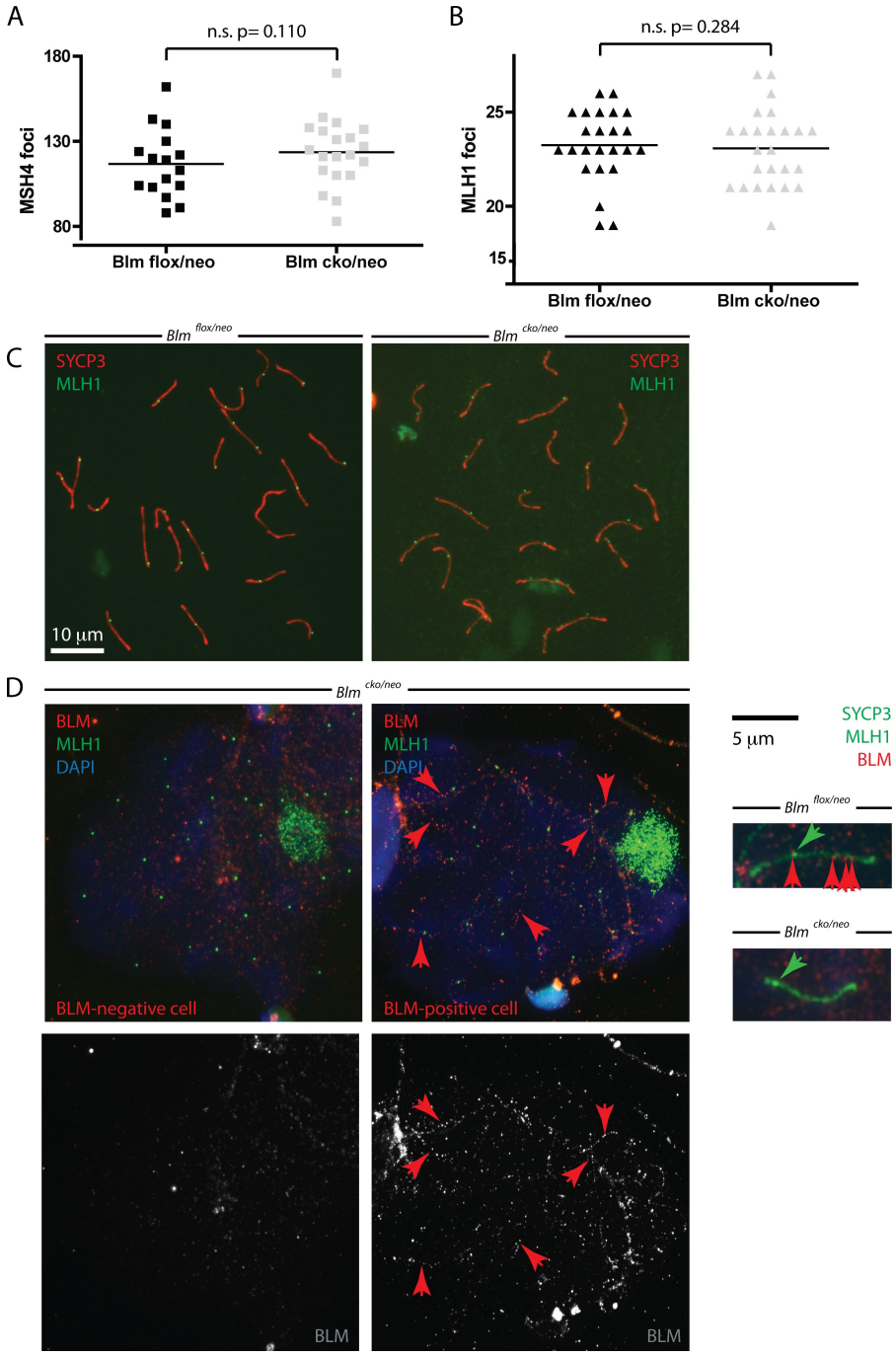

Figure 2. **Recombination intermediates in *Blm*$^{cko/neo}$ spermatocytes.** (A–C) Early and late recombination nodules appear in normal numbers (A and B) and with normal localization as measured by MSH4 (A) and MLH1 (B and C) foci counts. MSH4 and MLH1 foci were counted for *Blm*$^{flox/neo}$ (black) and *Blm*$^{cko/neo}$ (gray) mice. The mean values are represented by black horizontal lines. (C) Both *Blm*$^{flox/neo}$ (left) and *Blm*$^{cko/neo}$ (right) mice were stained with antibodies against SYCP3 (red) and MLH1 (green). (D) MLH1 localizes in cells with and without BLM localization. (left and middle) Dual staining of pachytene spermatocytes from *Blm*$^{cko/neo}$ mice with antibodies against MLH1 (green), BLM (red), and DAPI (blue) in the absence of any staining against synaptonemal complex proteins. BLM staining is absent in some cells from the CKO mouse (left) and present in other cells from the same mouse (middle, red arrows). MLH1 localization (green) is the same in both cohorts of cells. (right) Chromosome cores stained with both SYCP3 and MLH1 (green arrows) coupled with BLM (right, red arrows) show colocalization in the *Blm*$^{flox/neo}$ mouse; however, in the BLM-deleted mutant mouse where BLM is absent from some spermatocytes, MLH1 still localizes at a similar frequency to that of control animals.

chromatids (Bannister et al., 2004; Xu et al., 2005). Although not implying complete premature separation of sister chromatids, these data indicate partial loss of cohesion at these sites.

Blm$^{cko/neo}$ pachytene spermatocytes also show high levels of γH2AX staining at these regions of asynapsis (Fig. 5). This increased staining looks similar to γH2AX localization at the sex body in normal wild-type spermatocytes rather than the fainter, more-even staining seen at DSBs in wild-type cells. Some cells show one or two areas of strong γH2AX staining, (Fig. 5, left and middle), whereas other cells are almost completely covered by γH2AX staining. In the case of Fig. 5 (right), there are several wild-type pachytene cells surrounding a presumably BLM-deficient pachytene cell (Fig. 5). The BLM-deficient cell has several abnormal chromosome configurations, all of which are covered in γH2AX staining. Despite their obvious pairing defects, these asynaptic cells show normal MLH1 staining (unpublished data), suggesting that even when BLM deficiency results in mispairing, COs form normally.

Blm CKO mice show significant impairment in meiotic progression

Coupled with prophase I defects, *Blm* CKO mice showed significantly reduced testis size compared with controls, whereas other nontesticular tissues such as spleen and seminal vesicle showed no significant difference (Fig. 6 A). To determine any effect on sperm production in the CKO mice, epididymal

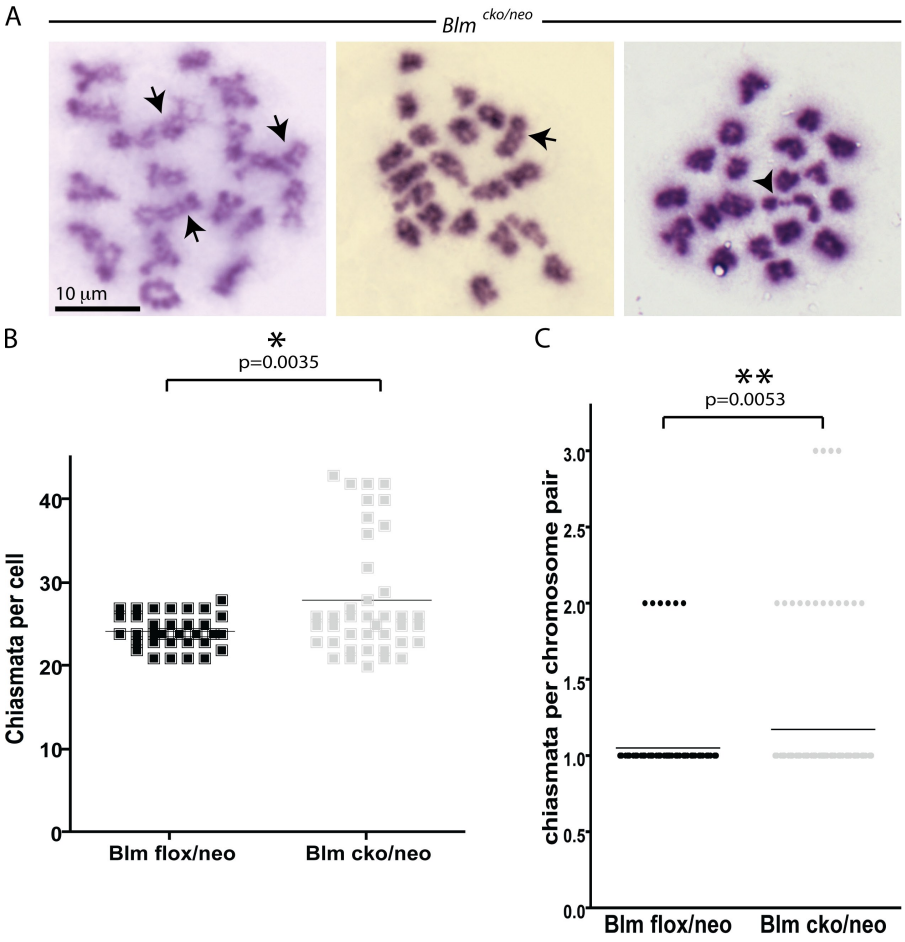

Figure 3. **Chiasmata-like structures are increased in *Blm* CKO cells.** (A) Diakinesis spreads from $Blm^{cko/neo}$ mice, shown by abnormal numbers of COs on single chromosomes (arrows) and structures between chromosomes (arrowhead). The mean values of chiasmata per cell counted from $Blm^{flox/neo}$ and $Blm^{cko/neo}$ mice showed a significant difference (*, P = 0.0035 by Welch's *t* test). (B) The number of chiasmata per individual chromosome pair was significantly different between the CKO and control (C) mice (**, P = 0.0053).

spermatozoa numbers were counted from $Blm^{flox/neo}$ and $Blm^{cko/neo}$ animals with the CKO mice having significantly fewer than the control mice (Fig. 6 B). To determine when this loss of cells is occurring, TUNEL staining was performed on both CKO and control testis sections. $Blm^{cko/neo}$ mice exhibit a significant increase in the number of apoptotic cells in the seminiferous tubules compared with $Blm^{flox/neo}$ mice (Fig. 7). The apoptotic cells appear to be in several different stages of spermatogenesis around prophase I/metaphase I. None of the cells appear to be dying in the spermatogonial stage, which would indicate a problem with premeiotic replication in BLM-deficient cells. This is reinforced by TUNEL staining in young premeiotic day 17 postpartum male testis sections, which show no significant difference between control and CKO mice, coupled with staining using the proliferating cell marker PCNA-1 and the germ cell nuclear antigen GCNA-1 (expressed in spermatogonia and spermatocytes) on adult and day 17 postpartum testis sections in which the $Blm^{cko/neo}$ testis sections appear similar to the $Blm^{flox/neo}$ sections (unpublished data). Thus, loss of BLM even in only a subset of spermatogonia does not impair mitotic proliferation on these cells, nor does it affect entry into meiosis.

To determine whether BLM-deficient cells were capable of completing meiosis, DNA was analyzed by PCR from testis, spermatozoa (extruded from the epididymis), tail, seminal vesicle, and spleen (not depicted) from both $Blm^{flox/neo}$ and $Blm^{cko/neo}$ animals for the presence of both the floxed allele and the conditionally deleted allele (Fig. 7). As expected, the floxed allele was identified in all tissues for both sets of mice (Fig. 7 H, two bands on the gel), whereas only DNA extracted from the testis of $Blm^{cko/neo}$ animals showed the presence of the deleted (CKO) band (Fig. 7 H, asterisks). Occasionally, a faint CKO band is apparent in the spermatozoa DNA and in DNA from seminal vesicle and spleen (unpublished data), and this reflects the leakiness of the CRE transgene driven by the *Tnap* promoter. Moreover, any faint band observed in the spermatozoa lane could be caused by the ~5% of nonspermatozoan epididymal cells, which includes a high proportion of blood cells. Thus, it is likely that the majority if not all mature spermatozoa in the epididymis of $Blm^{cko/neo}$ animals harbors only the floxed allele of *Blm.*

Discussion

Our analysis of prophase I events in *Blm*-CKO spermatocytes reveals normal progression of DSBR along the canonical CO pathway, as indicated by normal accumulation of RAD51, MSH4, MLH1, and MLH3 foci (Fig. 2 and not depicted), and apparently normal progression of synapsis and pairing, as demonstrated by the accumulation of SYCP3 and SYCP1 on meiotic chromosomes (Fig. 4). However, despite this, the absence of BLM results in altered synapsis figures, characterized by structures that are reminiscent of the multichromatid

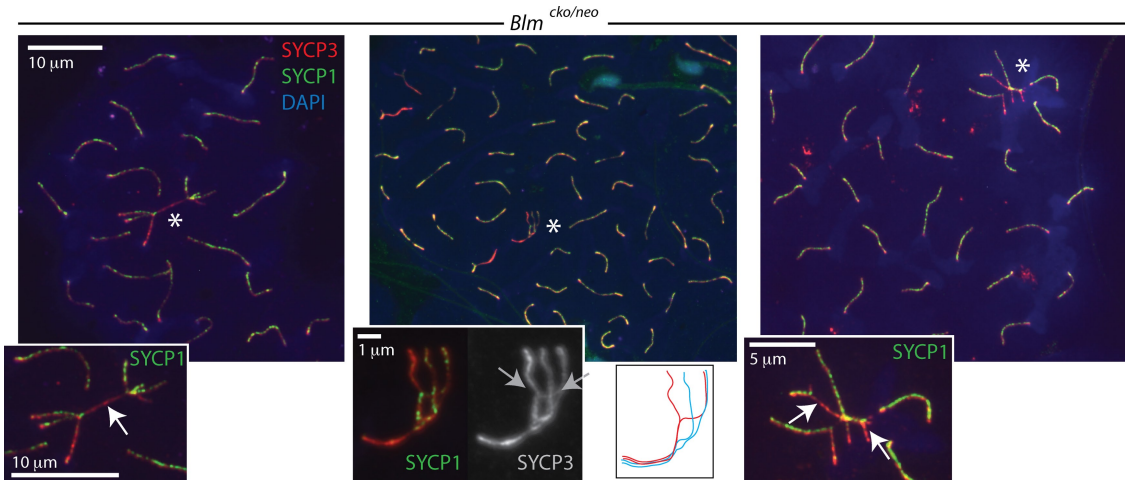

Figure 4. ***Blm*$^{cko/neo}$ spermatocytes show defects in synapsis.** Pachytene spermatocytes from *Blm*$^{cko/neo}$ mice stained with antibodies against synaptonemal complex proteins SYCP3 (red) and SYCP1 (green). Chromosomes displaying defective synapsis are shown by asterisks and in corresponding insets. Unsynapsed chromosomes that accumulate SYCP3 at the axial elements but not SYCP1 in the central element are shown by white arrows. Defective pairing, causing complex chromosome configurations not seen in wild-type pachynema, also occurs in *Blm*$^{cko/neo}$ (gray arrows). A cartoon is provided as a simple interpretation of this complex configuration, although other interpretations are also possible.

JMs (mcJMs) identified in *sgs1* yeast mutants (Fig. 4; Oh et al., 2007, 2008), and increased rates of mispairing and asynapsis in a subset of cells, as demonstrated by synapsis of multiple chromosomes of differing length and coincident localization of phosphorylated H2AX (Fig. 5). There is also evidence of limited precocious separation of sister chromatids, which become marked with SYCP3 and appear to be involved in these mcJM-like structures (Fig. 4). Moreover, the outcome of prophase I in *Blm* CKO mice is an increase in chiasmata or chiasmata-like structures at diakinesis in a subpopulation of spermatocytes (Fig. 3, A–C), leading us to conclude that these cells represent those in which BLM is absent. These data, coupled with the significant defects in meiotic progression in *Blm* CKO spermatocytes, lead us to the conclusion that BLM is absolutely necessary for normal completion of spermatogenesis and male fertility. Importantly, our data point to a specific requirement for BLM in meiotic events, whereas BLM appears to be dispensable for mitotic proliferation of spermatogonia before entry into prophase I. It is possible that other RecQ helicases, such as Werner's protein, may compensate for the loss of BLM during spermatogonial proliferation or that the rate of proliferation is increased to compensate for the loss of spermatogonia in the absence of BLM. However, the latter is unlikely because we see no overt increase in TUNEL-positive spermatogonia in *Blm* CKO males.

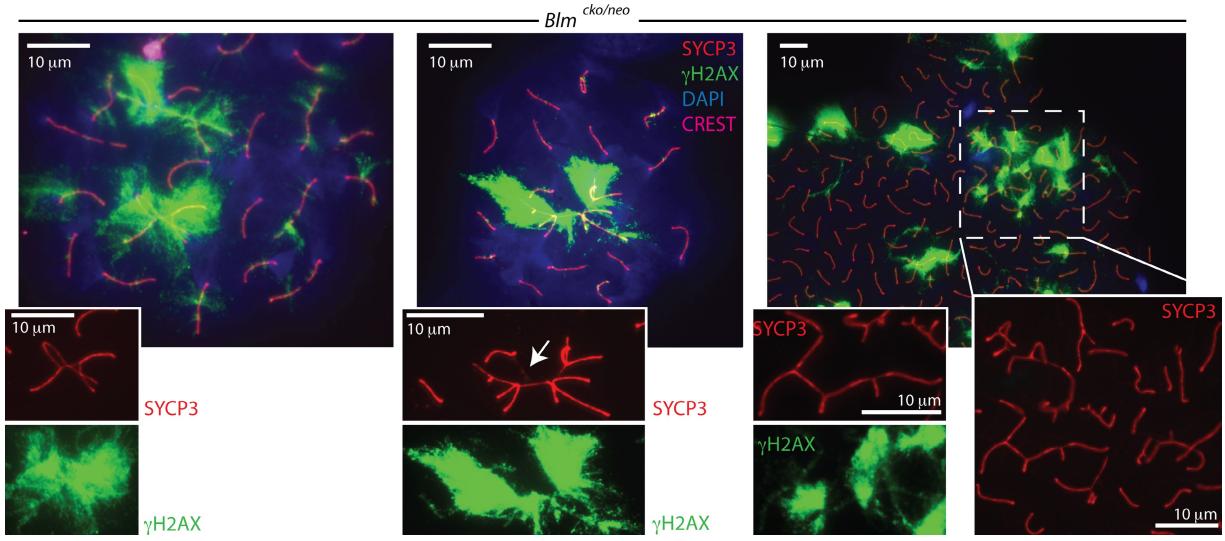

Figure 5. ***Blm*$^{cko/neo}$ spermatocytes show defects in γH2AX accumulation.** Spermatocytes from *Blm*$^{cko/neo}$ mice display abnormal γH2AX localization in pachynema when stained with antibodies against SYCP3 (red), γH2AX (green), DAPI (blue), and CREST (pink). γH2AX should be limited to the sex body and minor regions of accumulation on the chromosome cores at this stage in wild type (Fernandez-Capetillo et al., 2003); however, the staining in these cells is excessive. (insets) Enlarged regions of staining are shown. Note the complex chromatin configuration in the first two SYCP3 insets, and the bridge of SYCP3 staining is shown by the arrow. (right) A mass of cells stained similar to wild type, surrounding one cell showing complete overaccumulation of γH2AX and complex chromosome configurations. Dashed lines show the region that is enlarged in the indicated inset.

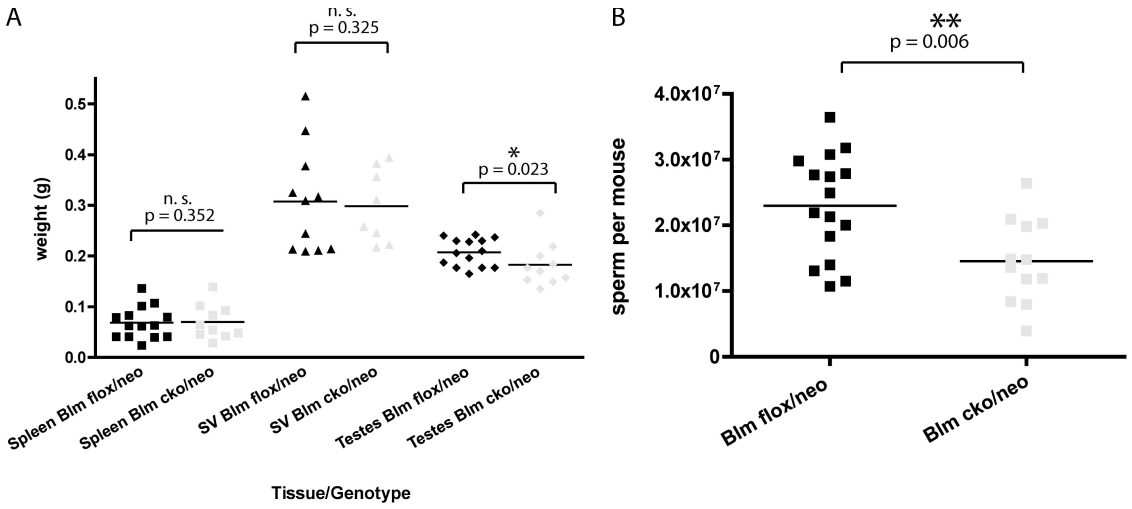

Figure 6. **Testes from $Blm^{cko/neo}$ mice show impaired growth and reduced spermatozoa compared with control littermates.** (A) Organ weights from both $Blm^{flox/neo}$ and $Blm^{cko/neo}$ mice. Spleen, seminal vesicle (SV), and testes weights from $Blm^{flox/neo}$ (black) and $Blm^{cko/neo}$ (gray) animals. Although spleen and seminal vesicle weights were not significantly different between the two genotypes (P = 0.352 and P = 0.325, respectively), testes weights were significantly lower in $Blm^{cko/neo}$ mice (mean testes weights of 649 mg and 723 mg, respectively; *, P = 0.023). (B) Sperm number per animal was significantly reduced in $Blm^{cko/neo}$ animals compared with $Blm^{flox/neo}$ mice (means of 1.456×10^7 and 2.297×10^7, respectively; **, P = 0.006). Mean values for each group are shown by the black lines, with significance indicated by asterisks.

Collectively, these data represent the first analysis of BLM function in mammalian meiosis and indicate that BLM is playing a critical role by (a) preventing nonhomologous synapsis, (b) eliminating aberrant CO events before exit from prophase I, and/or (c) by preventing mcJM events. In the first instance, it is important to note that abnormal synapsis events in *Blm* CKO spermatocytes occur despite apparently intact DSBR, assuming that RAD51, MSH4, and MLH1 profiles can be regarded as an accurate profile of DSBR via the major MSH4–MSH5 and MLH1–MLH3 pathways. This suggests that in mice, BLM can prevent nonhomologous synapsis via a mechanism that does not affect the major DSBR pathway for CO formation.

The second important finding from our data is that BLM modulates final chiasmata frequency because a subset of spermatocytes from *Blm*-conditional males exhibits increased physical associations. Given that MLH1–MLH3 focus frequency is normal in *Blm* CKO cells, the additional chiasmata or chiasmata-like structures must arise through mechanisms that do not directly involve MLH1–MLH3.

Third, our data indicate that the absence of BLM results in the mcJMs or aberrant chromosome configurations reminiscent of mcJM events described in budding yeast (Oh et al., 2007), representing the first cytogenetic observation of such structures in any mammalian species (Fig. 4, middle; and Fig. 5, left). Coupled with this observation are the data showing an increase in BLM foci in the absence of MLH3. Collectively, these results indicate that BLM may participate in preventing or resolving such mcJM structures and that the canonical DSBR pathway involving MSH4–MSH5 and MLH1–MLH3 may act to suppress the appearance of such structures. However, what remains unclear is how the absence of MLH3 specifically at sites of crossing over may affect the deposition of BLM foci at more than just these sites during prophase because our observations reveal hyperaccumulation of BLM foci at pachynema in spermatocytes from $Mlh3^{-/-}$ males (Fig. 1). An alternative explanation for these aberrant synapsis figures is that they represent nonallelic interactions possibly at genome regions that are rich in dispersed repeats. However, the configurations evident in these cells appear to involve SCs of similar length (Fig. 4, middle), so it is more likely that these synapsis events involve allelic regions. More likely, the aberrant synapsis events may also be heterogeneous in nature, involving multiple types of association.

Recent studies from our laboratory have implicated MUS81 endonuclease as a minor alternative pathway for the processing of DSBs into CO events (Holloway et al., 2008). Although controversy still remains as to the nature of the role for MUS81 in CO control, our analysis of *Mus81* homozygous mutant animals revealed defects in prophase I, including an up-regulation and persistence of BLM in $Mus81^{-/-}$ pachytene cells, which is similar to that seen for $Mlh3^{-/-}$ males in this study (Holloway et al., 2008). Collectively with the fact that mammalian BLM and MUS81 have been shown to interact in vitro (Zhang et al., 2005) and the data from yeast showing synthetic lethality of *sgs1* and *mus81/mms4* mutants (Jessop and Lichten, 2008; Oh et al., 2008), these data suggest that this minor pathway interacts with BLM to regulate the processing of DSB intermediates, aberrant or otherwise. Because of the lack of appropriate functional antibodies against MUS81, we are precluded from studying the physical association between these two proteins during prophase I.

The suggestion that the antirecombinational and synapsis roles of BLM during meiosis are confined to non-ZMM repair pathways is in line with recent studies in *Saccharomyces cerevisiae*. Yeast *sgs1* mutants display only modest increases in Cos; however, it is clear that the elevated COs represent ectopic and/or aberrant events (Rockmill et al., 2003; Jessop et al., 2006; Oh et al., 2007, 2008; Jessop and Lichten, 2008). Importantly, Oh et al. (2007) report a small 1.14-fold increase in CO rates in *sgs1* mutant yeast coupled with an ~35% increase in all classes

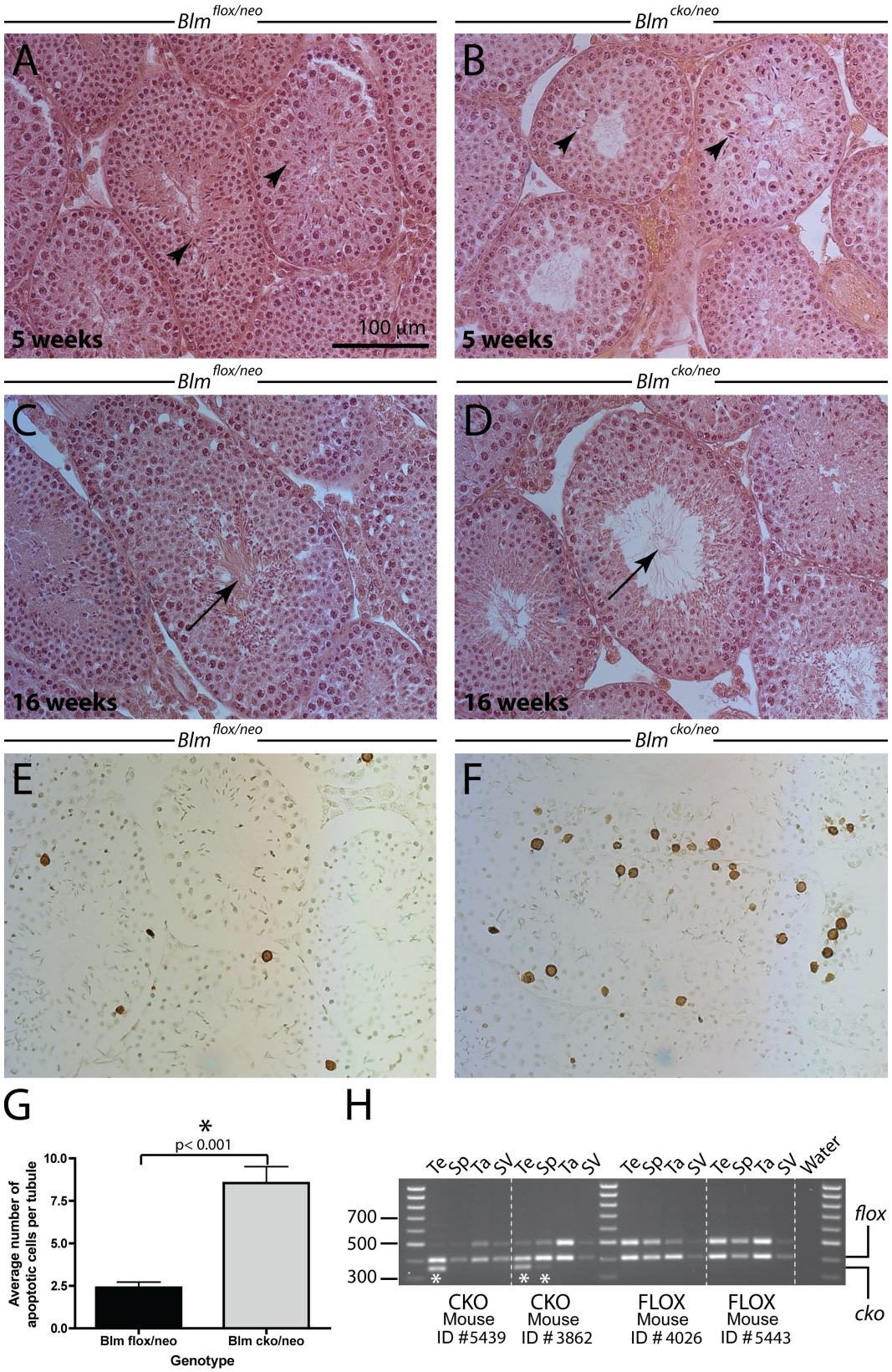

Figure 7. **BLM-deficient cells undergo apoptosis during spermatogenesis.** (A–D) H&E staining of histological sections from both $Blm^{flox/neo}$ (A and C) and $Blm^{cko/neo}$ (B and D) mice at either 5 (A and B) or 16 wk (C and D) of age. (A and B) Spermatids are present in both genotypes of mice at 5 wk, although fewer were in the $Blm^{cko/neo}$ mice (arrowheads). (B) The seminiferous tubules are also less densely packed with cells in the $Blm^{cko/neo}$ mice. (C and D) By 16 wk of age, sperm tails are evident in the lumen of both the $Blm^{flox/neo}$ (C) and $Blm^{cko/neo}$ (D; arrows) although, fewer were in the $Blm^{cko/neo}$ sections. (E–G) TUNEL staining of testes sections from $Blm^{flox/neo}$ (E) and $Blm^{cko/neo}$ (F) mice reveals a significant increase in apoptotic cells in the $Blm^{cko/neo}$ testes (G, gray bar) compared with $Blm^{flox/neo}$ (8.6 and 2.4 apoptotic cells per tubule, respectively; *, $P < 0.0001$). Error bars show the SEM, and the asterisk indicates significance.

of JMs, the majority of which are those involving three or four chromatids. The combinatorial effect of mutations in *Sgs1* with mutations in *ZMM* genes reveals that *sgs1* partially suppresses the CO phenotype of *zmm* mutants. Thus, much higher CO rates are observed in *sgs1msh4* double mutants than *msh4* single mutants to essentially normal wild-type levels but not to the levels seen in *sgs1* mutants (Jessop et al., 2006; Oh et al., 2007). This suggests that the RecQ helicase antagonizes the ZMM-dependent pathway for accurate CO formation. Indeed, as proposed by Jessop et al. (2006), one function of the ZMM group may be to prevent access of Sgs1 to CO intermediates possibly indirectly through actions on other components of the Sgs1 complex (Top3 or Rmi1; Mullen et al., 2005), thereby suppressing the antirecombination activity of the helicase complex at these sites. This suggestion is in line with data presented herein showing that BLM helicase accumulates on mouse chromosomes in the absence of MLH3. These data are confounded by the effects of mutations in BLM orthologues in other species, namely *Drosophila melanogaster mus309*, *Schizosaccharomyces pombe rqh1*, and *Caenorhabditis elegans him-6*. Mutation of these genes results in a significant decrease in meiotic crossing over, as much as 46% in *Drosophila* females (McVey et al., 2004) coupled with an increase in mitotic recombination in *Drosophila* and *S. pombe* (Adams et al., 2003; McVey et al., 2004; Cromie et al., 2008). The difference between function of BLM/Sgs1 and that of Rqh1 in *S. pombe* may be explained by the absence of the ZMM pro-CO proteins in fission yeast meiosis and the predominance instead of the Mus81–Eme1 CO pathway (Boddy et al., 2001). In yeast and mouse, the presence of the ZMM factors may prevent Sgs1/BLM access to intermediate JM structures, except those aberrant structures to which MLH1–MLH3 do not bind, allowing accumulation of Sgs1/BLM to drive repair through a Mus81-mediated process (Oh et al., 2007). Consequently, in the absence of ZMM factors in fission yeast, Rqh1 may be driving repair of single-Holliday junction intermediates through a Mus81-dependent process. Thus, it may be the presence or absence of the ZMM pathway that dictates the functional activity of the RecQ helicase in different meiotic species. These discrepancies between Sgs1/BLM function in yeast, flies, worms, and mice underscore the importance of studying RecQ helicase in multiple organisms, especially mice, as they are most closely related to humans.

Collectively, our data reveal an important role for BLM helicase in mammalian meiosis that was predicted by its localization on meiotic chromosomes during prophase I. By overcoming the technical challenges of incomplete CRE-mediated excision in *Blm* CKO mice, we find that, similar to budding yeast, mouse BLM is essential for mediating divergent recombination pathways and appears to act to direct repair of complex chromosome structures that are not conventionally repaired by the DSBR machinery. The complex interactions between BLM helicase and this ZMM pathway, as well as between BLM and MUS81, merit further investigation in the mouse because it is clear that different recombination strategies require different degrees of BLM input.

Materials and methods

Mouse mutant strains and breeding

All mouse experiments were conducted with the prior approval of the Cornell Institutional Animal Care and Use Committee. We obtained mice (provided by P. Leder, Harvard University, Boston, MA) with a floxed *Blm* exon 8–conditional allele (termed $Blm^{Tm4Ches}$) and mice with the full null allele as a result of the insertion of a neo cassette into the *Blm* gene (termed $Blm^{Tm2Ches}$; Chester et al., 2006). When bred with a *Tnap-cre* (tissue-nonspecific alkaline phosphatase expressed in primordial germ cells; Lomelí et al., 2000)–expressing mouse, the floxed allele was excised in those tissues to generate an exon 8 deletion allele (termed $Blm^{Tm3Ches}$). For simplicity, we will refer to the floxed allele as Blm^{flox}, the null allele as Blm^{neo}, and the conditionally deleted allele as Blm^{cko}. We bred female $Blm^{flox/flox}$ or $Blm^{flox/WT}$ mice with male $Blm^{WT/neo}$ *Tnap-cre*$^{+}$. This produced experimental mice with the genotype $Blm^{cko/neo}$ and control mice $Blm^{flox/neo}$ *Tnap-cre*$^{-}$. We also generated control mice $Blm^{WT/neo}$ *Tnap-cre*$^{+}$, which have no floxed allele. All of the experiments described in this study were performed using these two cohorts of negative control mice, so as to ascertain the effect that CRE might have on spermatogenesis in the mice. Because the two control groups did not yield significantly different results from each other, only the $Blm^{flox/neo}$ mice are presented in this study as comparisons with $Blm^{neo/cko}$ mice. Mice were genotyped for *Blm* alleles as previously described (Chester et al., 2006).

PCR analysis of *Blm* deletion

DNA was extracted from several tissues, including testis, spermatozoa extruded from the epididymis (containing some contaminating blood cells), tail, and seminal vesicle, and was subjected to dual PCR for the floxed allele and the CKO allele. Each PCR reaction began with 30 ng DNA, and the following cycling conditions were used: 94°C for 2 min; 35 cycles of 94°C for 15 s, 59.5°C for 15 s, and 72°C for 30 s; 72°C for 1 min; and 22°C hold.

Sperm counts

Mature spermatozoa were quantified by extracting the caudal epididymides, puncturing, and incubating in media containing 4% BSA for 20 min to allow the sperm to swim out. 20 µl media was added to 480 µl 10% formalin to fix the sperm, and the cells were counted using a hemocytometer.

Histology and TUNEL staining

Testes were removed from mice, fixed overnight in 10% formalin at 4°C, and washed in three changes of 70% ethanol over a period of 48 h. Fixed tissues were cut into 4-µm sections and stained appropriately. TUNEL staining was performed using a TUNEL staining kit (Apoptag; Millipore).

Chromosome spreading and immunofluorescent staining

Tubules were minced in sucrose solution and fixed onto slides in 1% paraformaldehyde over a period of 3 h in a humidified chamber. Slides were washed in 1× PBS with photoflo (Kodak) and 1× PBS containing 0.1% Triton X-100 and blocked in 10% goat serum. They were stained with primary antibodies against SYCP3 (at a concentration of 1:5,000) in conjunction with BLM (1:100), MLH1 (1:50; BD), SYCP1 (1:500), MSH4 (1:500), or γH2AX (1:10,000) and in conjunction with centromere staining using CREST antiserum. BLM antibody was provided by

(H) PCR analysis of several tissues (Te, testis; Sp, spermatozoa extruded from the epididymis; Ta, Tail; SV, seminal vesicle) from two $Blm^{cko/neo}$ (CKO mouse ID no. 5439 and 3862) and two $Blm^{flox/neo}$ (CKO mouse ID no. 4026 and 5443) mice. PCR amplification of the floxed allele produces two higher molecular mass bands (~500 and 400 bp) present in all tissues from both genotypes, whereas the CKO (or deleted) allele is present almost exclusively in the testes of the $Blm^{cko/neo}$ mice (small band at ~350 bp). Some leaky expression of the *Cre* results in a faint *cko* band in seminal vesicle, tail, and occasionally in the cells of the epididymal extrusion (which contains some contaminating blood cells in addition to spermatozoa). Thus, the presence of the *cko*-deleted band in the spermatozoa lane of the second CKO mouse (ID no. 3862) may represent leaky *Cre* expression in blood cells or some persistent CKO spermatozoa (asterisks). Marker sizes are shown on the left.

R. Freire (University Hospital of the Canary Islands, Tenerife, Spain), and the MSH4 antibody was provided by T. Ashley (Yale University, New Haven, CT). Alexa Fluor Cy3–, Cy5–, and FITC–conjugated secondary antibodies were used (Invitrogen) for immunofluorescent staining at 37°C for 1 h. Slides were washed and mounted with Prolong gold antifade (Invitrogen). Primary antibodies and conditions used in this study were described previously (Lipkin et al., 2002; Kolas et al., 2005; Holloway et al., 2008); however, for the dual labeling of MLH1 and SYCP3 using the same fluorochrome-labeled secondary antibody, the primary SYCP3 antibody was used at a concentration of 1:50,000 as previously described (Lipkin et al., 2002).

Diakinesis chromosome spreading

This procedure was described previously (Holloway et al., 2008). In brief, testes were minced in hypotonic buffer, and the large clumps were removed and incubated at room temperature for 20 min. The cell suspension was centrifuged, and the supernatant was removed. Cells were fixed in a methanol/acetic acid/chloroform fixative, centrifuged again, and resuspended in methanol/acetic acid. Fixed cells were dropped onto slides, dried quickly, and stained with Giemsa.

Image acquisition

All slides were visualized using a microscope (Imager Z1; Carl Zeiss, Inc.) under a 20× 0.5 NA ECPlan Neofluar air immersion (Carl Zeiss, Inc.) or 63× 1.4 NA Plan Apochromat oil immersion differential interference contrast (Carl Zeiss, Inc.) magnifying objective at room temperature. The fluorochromes used were Alexa Fluor labeled with Cy3, Cy5, or FITC. Images were captured with a cooled charged-coupled device camera (AxioCam MRm; Carl Zeiss, Inc.) and processed using AxioVision software (version 4.7.2; Carl Zeiss, Inc.).

We acknowledge the generosity of Drs. Nicholas Chester and Philip Leder for providing the two alleles of *Blm* mice, Dr. Jeremy Wang (University of Pennsylvania, Philadelphia, PA) for the *Tnap-Cre* mice (originally obtained from the laboratory of Dr. Andras Nagy, University of Toronto, Toronto, Ontario, Canada), Dr. Terry Ashley for providing the anti-MSH4 antibody, and Dr. Ramundo Freire for providing the anti-BLM antibody. We thank our colleagues, Drs. Eric Alani, Mark Roberson, and Robert Weiss for critical comments and helpful suggestions.

This work is supported by a postdoctoral fellowship from the Hereditary Diseases Foundation (to J.K. Holloway) and by the National Institutes of Health (grant HD41012 to P.E. Cohen).

Submitted: 8 September 2009
Accepted: 23 February 2010

References

Adams, M.D., M. McVey, and J.J. Sekelsky. 2003. *Drosophila* BLM in double-strand break repair by synthesis-dependent strand annealing. *Science.* 299:265–267. doi:10.1126/science.1077198

Bannister, L.A., L.G. Reinholdt, R.J. Munroe, and J.C. Schimenti. 2004. Positional cloning and characterization of mouse mei8, a disrupted allelle of the meiotic cohesin Rec8. *Genesis.* 40:184–194. doi:10.1002/gene.20085

Bishop, D.K., and D. Zickler. 2004. Early decision; meiotic crossover interference prior to stable strand exchange and synapsis. *Cell.* 117:9–15. doi:10.1016/S0092-8674(04)00297-1

Boddy, M.N., P.H. Gaillard, W.H. McDonald, P. Shanahan, J.R. Yates III, and P. Russell. 2001. Mus81-Eme1 are essential components of a Holliday junction resolvase. *Cell.* 107:537–548. doi:10.1016/S0092-8674(01)00536-0

Börner, G.V., N. Kleckner, and N. Hunter. 2004. Crossover/noncrossover differentiation, synaptonemal complex formation, and regulatory surveillance at the leptotene/zygotene transition of meiosis. *Cell.* 117:29–45. doi:10.1016/S0092-8674(04)00292-2

Chester, N., F. Kuo, C. Kozak, C.D. O'Hara, and P. Leder. 1998. Stage-specific apoptosis, developmental delay, and embryonic lethality in mice homozygous for a targeted disruption in the murine Bloom's syndrome gene. *Genes Dev.* 12:3382–3393. doi:10.1101/gad.12.21.3382

Chester, N., H. Babbe, J. Pinkas, C. Manning, and P. Leder. 2006. Mutation of the murine Bloom's syndrome gene produces global genome destabilization. *Mol. Cell. Biol.* 26:6713–6726. doi:10.1128/MCB.00296-06

Cromie, G.A., R.W. Hyppa, and G.R. Smith. 2008. The fission yeast BLM homolog Rqh1 promotes meiotic recombination. *Genetics.* 179:1157–1167. doi:10.1534/genetics.108.088955

de Vries, S.S., E.B. Baart, M. Dekker, A. Siezen, D.G. de Rooij, P. de Boer, and H. te Riele. 1999. Mouse MutS-like protein Msh5 is required for proper chromosome synapsis in male and female meiosis. *Genes Dev.* 13:523–531. doi:10.1101/gad.13.5.523

Edelmann, W., P.E. Cohen, B. Kneitz, N. Winand, M. Lia, J. Heyer, R. Kolodner, J.W. Pollard, and R. Kucherlapati. 1999. Mammalian MutS homologue 5 is required for chromosome pairing in meiosis. *Nat. Genet.* 21:123–127. doi:10.1038/5075

Ellis, N.A., and J. German. 1996. Molecular genetics of Bloom's syndrome. *Hum. Mol. Genet.* 5:1457–1463.

Fernandez-Capetillo, O., S.K. Mahadevaiah, A. Celeste, P.J. Romanienko, R.D. Camerini-Otero, W.M. Bonner, K. Manova, P. Burgoyne, and A. Nussenzweig. 2003. H2AX is required for chromatin remodeling and inactivation of sex chromosomes in male mouse meiosis. *Dev. Cell.* 4:497–508. doi:10.1016/S1534-5807(03)00093-5

German, J. 1993. Bloom syndrome: a mendelian prototype of somatic mutational disease. *Medicine (Baltimore).* 72:393–406.

German, J. 1995. Bloom's syndrome. *Dermatol. Clin.* 13:7–18.

Holloway, J.K., J. Booth, W. Edelmann, C.H. McGowan, and P.E. Cohen. 2008. MUS81 generates a subset of MLH1-MLH3-independent crossovers in mammalian meiosis. *PLoS Genet.* 4:e1000186. doi:10.1371/journal.pgen.1000186

Jessop, L., and M. Lichten. 2008. Mus81/Mms4 endonuclease and Sgs1 helicase collaborate to ensure proper recombination intermediate metabolism during meiosis. *Mol. Cell.* 31:313–323. doi:10.1016/j.molcel.2008.05.021

Jessop, L., B. Rockmill, G.S. Roeder, and M. Lichten. 2006. Meiotic chromosome synapsis-promoting proteins antagonize the anti-crossover activity of sgs1. *PLoS Genet.* 2:e155. doi:10.1371/journal.pgen.0020155

Kauli, R., R. Prager-lewin, H. Kaufman, and Z. Laron. 1977. Gonadal function in Bloom's syndrome. *Clin. Endocrinol. (Oxf.).* 6:285–289. doi:10.1111/j.1365-2265.1977.tb02013.x

Kneitz, B., P.E. Cohen, E. Avdievich, L. Zhu, M.F. Kane, H. Hou Jr., R.D. Kolodner, R. Kucherlapati, J.W. Pollard, and W. Edelmann. 2000. MutS homolog 4 localization to meiotic chromosomes is required for chromosome pairing during meiosis in male and female mice. *Genes Dev.* 14:1085–1097.

Kolas, N.K., A. Svetlanov, M.L. Lenzi, F.P. Macaluso, S.M. Lipkin, R.M. Liskay, J. Greally, W. Edelmann, and P.E. Cohen. 2005. Localization of MMR proteins on meiotic chromosomes in mice indicates distinct functions during prophase I. *J. Cell Biol.* 171:447–458. doi:10.1083/jcb.200506170

Lipkin, S.M., P.B. Moens, V. Wang, M. Lenzi, D. Shanmugarajah, A. Gilgeous, J. Thomas, J. Cheng, J.W. Touchman, E.D. Green, et al. 2002. Meiotic arrest and aneuploidy in MLH3-deficient mice. *Nat. Genet.* 31:385–390.

Lomelí, H., V. Ramos-Mejía, M. Gertsenstein, C.G. Lobe, and A. Nagy. 2000. Targeted insertion of Cre recombinase into the TNAP gene: excision in primordial germ cells. *Genesis.* 26:116–117. doi:10.1002/(SICI)1526-968X(200002)26:2<116::AID-GENE4>3.0.CO;2-X

McVey, M., J.R. Larocque, M.D. Adams, and J.J. Sekelsky. 2004. Formation of deletions during double-strand break repair in *Drosophila* DmBlm mutants occurs after strand invasion. *Proc. Natl. Acad. Sci. USA.* 101:15694–15699. doi:10.1073/pnas.0406157101

Moens, P.B., R. Freire, M. Tarsounas, B. Spyropoulos, and S.P. Jackson. 2000. Expression and nuclear localization of BLM, a chromosome stability protein mutated in Bloom's syndrome, suggest a role in recombination during meiotic prophase. *J. Cell Sci.* 113:663–672.

Mullen, J.R., F.S. Nallaseth, Y.Q. Lan, C.E. Slagle, and S.J. Brill. 2005. Yeast Rmi1/Nce4 controls genome stability as a subunit of the Sgs1-Top3 complex. *Mol. Cell. Biol.* 25:4476–4487. doi:10.1128/MCB.25.11.4476-4487.2005

Oh, S.D., J.P. Lao, P.Y. Hwang, A.F. Taylor, G.R. Smith, and N. Hunter. 2007. BLM ortholog, Sgs1, prevents aberrant crossing-over by suppressing formation of multichromatid joint molecules. *Cell.* 130:259–272. doi:10.1016/j.cell.2007.05.035

Oh, S.D., J.P. Lao, A.F. Taylor, G.R. Smith, and N. Hunter. 2008. RecQ helicase, Sgs1, and XPF family endonuclease, Mus81-Mms4, resolve aberrant joint molecules during meiotic recombination. *Mol. Cell.* 31:324–336. doi:10.1016/j.molcel.2008.07.006

Paquis-Flucklinger, V., S. Santucci-Darmanin, R. Paul, A. Saunières, C. Turc-Carel, and C. Desnuelle. 1997. Cloning and expression analysis of a meiosis-specific MutS homolog: the human MSH4 gene. *Genomics.* 44:188–194. doi:10.1006/geno.1997.4857

Payne, M., and I.D. Hickson. 2009. Genomic instability and cancer: lessons from analysis of Bloom's syndrome. *Biochem. Soc. Trans.* 37:553–559. doi:10.1042/BST0370553

Rockmill, B., J.C. Fung, S.S. Branda, and G.S. Roeder. 2003. The Sgs1 helicase regulates chromosome synapsis and meiotic crossing over. *Curr. Biol.* 13:1954–1962. doi:10.1016/j.cub.2003.10.059

Shinohara, A., and M. Shinohara. 2004. Roles of RecA homologues Rad51 and Dmc1 during meiotic recombination. *Cytogenet. Genome Res.* 107:201–207. doi:10.1159/000080598

Shinohara, M., S.D. Oh, N. Hunter, and A. Shinohara. 2008. Crossover assurance and crossover interference are distinctly regulated by the ZMM proteins during yeast meiosis. *Nat. Genet.* 40:299–309. doi:10.1038/ng.83

Walpita, D., A.W. Plug, N.F. Neff, J. German, and T. Ashley. 1999. Bloom's syndrome protein, BLM, colocalizes with replication protein A in meiotic prophase nuclei of mammalian spermatocytes. *Proc. Natl. Acad. Sci. USA.* 96:5622–5627. doi:10.1073/pnas.96.10.5622

Wu, L., C.Z. Bachrati, J. Ou, C. Xu, J. Yin, M. Chang, W. Wang, L. Li, G.W. Brown, and I.D. Hickson. 2006. BLAP75/RMI1 promotes the BLM-dependent dissolution of homologous recombination intermediates. *Proc. Natl. Acad. Sci. USA.* 103:4068–4073. doi:10.1073/pnas.0508295103

Xu, H., M.D. Beasley, W.D. Warren, G.T. van der Horst, and M.J. McKay. 2005. Absence of mouse REC8 cohesin promotes synapsis of sister chromatids in meiosis. *Dev. Cell.* 8:949–961. doi:10.1016/j.devcel.2005.03.018

Yin, J., A. Sobeck, C. Xu, A.R. Meetei, M. Hoatlin, L. Li, and W. Wang. 2005. BLAP75, an essential component of Bloom's syndrome protein complexes that maintain genome integrity. *EMBO J.* 24:1465–1476. doi:10.1038/sj.emboj.7600622

Zhang, R., S. Sengupta, Q. Yang, S.P. Linke, N. Yanaihara, J. Bradsher, V. Blais, C.H. McGowan, and C.C. Harris. 2005. BLM helicase facilitates Mus81 endonuclease activity in human cells. *Cancer Res.* 65:2526–2531. doi:10.1158/0008-5472.CAN-04-2421